Muon spin relaxation study of solute–vacancy interactions during natural aging of Al–Mg–Si–Cu alloys

Sigurd Wenner[1]*, Calin D. Marioara[1], Katsuhiko Nishimura[2], Kenji Matsuda[2], Seungwon Lee[2], Takahiro Namiki[2], Isao Watanabe[3], Teiichiro Matsuzaki[3], and Randi Holmestad[4]
[1] Materials and Nanotechnology, SINTEF Industry, N-7491 Trondheim, Norway.
[2] Graduate School of Science and Engineering, University of Toyama, Toyama 930-8555, Japan.
[3] RIKEN Nishina Center for Accelerator Based Science, Wako, 351-0198, Japan
[4] Department of Physics, NTNU, N-7491Trondheim, Norway

* Corresponding author. E-mail: sigurd.wenner@sintef.no

Abstract

Muon spin relaxation has the unique ability to detect very low concentrations of vacancies and vacancy–solute complexes in solids. In this work, we investigate quaternary Al–Mg–Si–Cu alloys and show that after quenching to room temperature from 848 K (575 °C), vacancies gradually become incorporated into clusters in the Al matrix. The total amount of vacancies in the material increases as small vacancy-rich clusters are formed, which is the opposite of the behavior in Cu-free Al–Mg–Si alloys.

Keywords: Aluminium alloys; Al-Mg-Si-Cu; Muon spin relaxation; Atomic clustering; Vacancies

Age-hardenable aluminium alloys are strengthened by nanometer-sized atomic clusters and precipitates that are coherent with the aluminium matrix. These are formed by the segregation of atoms (e.g. Mg and Si), from a solid solution where the solute atoms occupy substitutional sites in fcc-Al. Such a solid solution comprising a few % of alloying elements is achieved by solution heat treatment (SHT) – an annealing step in the range 773–873 K (500–600 °C). The solid solution is highly unstable after rapid cooling from SHT. During further lower-temperature heat treatments (artificial aging) and even room temperature storage (natural aging), vacancies and solute atoms co-diffuse and order to produce atomic clusters, still with all atoms at fcc-Al positions [1-3]. In Al–Mg–Si (6xxx) alloys, this process is extremely complicated and consist of many distinct stages happening over a wide range of time scales, from seconds to years [4-6]. Minor additions of certain elements to the alloy composition can modify the properties of the alloy. The most important quaternary element in an industrial context is copper, as it enhances the precipitate nucleation and increases the hardness in Al–Mg–Si alloys. New types of precipitate phases are also formed with the introduction of Cu [7-9], and Cu has been found to suppress the detrimental effect of room temperature storage between SHT and artificial aging [4, 10-11].

The most important techniques to detect and quantify precipitates in the 6xxx system has been transmission electron microscopy (TEM) and atom probe tomography (APT). However, small atomic clusters are difficult to detect in TEM, APT is not suitable to investigate the crystallography of precipitates, and neither technique can map the presence of vacancies. Studying the microstructure shortly after quenching from SHT is also very challenging with these techniques, and requires sophisticated approaches [12]. Therefore, despite being a well-studied system, the clustering and precipitation in Al–Mg–Si alloys poses many unanswered questions which require unconventional techniques to be answered.

Muon spin relaxation (μSR) is one such technique, which relies on the production of exotic particles (positive muons) for investigating short-range magnetic fields and the presence of point defects in solids. When a high-energy muon enters a sample of aluminium, it is thermalized in a few picoseconds, and proceeds to diffuse interstitially inside the sample. If the muon is trapped at a certain site and therefore stationary, the magnetic dipole interaction between the magnetic moment of the muon and the nuclear magnetic moment of ^{27}Al causes precession of the muon spin, and in time the gradual depolarization (relaxation) of an ensemble of muon spins [13-14]. The relaxation rate gives us information on the particular trapping site and the trapping–detrapping kinetics, enabling the identification of various point defects in differently heat-treated alloy samples. This work builds upon earlier literature on aluminium with trace elements and Al–Mg–Si alloys and extends the analysis to the same alloys with Cu additions. The Al–Mg–Si–Cu alloys show a surprising muon trapping behavior that does not occur without all three alloying elements present. This discovery helps to further our understanding of the vacancy and clustering kinetics during natural aging in Al–Mg–Si(–Cu) alloys.

The materials used in this study were prepared by melting pure Al (purity 99.99 %) with Si and Mg (purity 99.9 %) and Cu (purity 99.99 %) in air. The resulting ingots were formed into 1.0 mm thick plates by hot and cold rolling. Several pieces of the samples were cut out from the plate with the approximate dimensions 1.0 × 25 × 25 mm^3. The

chemical compositions and heat treatment temperatures/periods are described in Table 1. All the samples underwent a SHT at 848 K (575 ºC) for 1 hour and a subsequent quenching in ice water. After quenching, three kinds of treatments were employed:

1. The μSR measurement started immediately after quenching from SHT (within approximately 15 min). The datasets with this process are denoted *-AQ.
2. Samples were stored at room temperature for a number of days before the measurement (denoted as *-…d).
3. Immediately after quenching, samples were annealed at a given temperature in the range 373–623 K (100–350 ºC) for a time required to stabilize the precipitate microstructure (noted as *-…C).

Since the base aluminum used in this study contains a few ppm of trace elements such as Si, Fe, Cu, Mn and Mg, we also measured the temperature dependence of μSR spectra with base Al to estimate the background trapping rate level from impurities.

The μSR experiments were carried out at the RIKEN-RAL Muon Facility at the Rutherford–Appleton laboratory [15]. A pulsed positive muon beam is produced via the decay of positive pions, which are a product of nuclear reactions between a carbon target and high-energy protons from the ISIS synchrotron. The muons are 100% spin polarized antiparallel to their velocity. Each muon decays into a positron and two neutrinos. The emission direction of the positron is asymmetric with respect to the muon spin. The probability of emission in a certain direction is $P(\theta) = 1 + A\cos(\theta)$, in which θ is the angle between the positron direction and the muon spin, and A is an asymmetry parameter. We used the ARGUS muon spectrometer, which detects positrons in the forward and backward direction with respect to the incoming muon beam. From this we obtain the degree of muon spin relaxation (or simply *asymmetry*) as a function of time spent inside the material before decaying.

Since muon kinetics vary greatly with temperature, a helium flow cryostat was used to control the temperature of the samples. Temperature series were acquired, with 20 to 60 million positron counts (events) recorded at each temperature point in the range 20–300 K (−253 to +27 °C). In isothermal measurements, as quenched (AQ) samples were kept at 280 K (7 °C), and 10 million positron counts were recorded at each time step to monitor the time evolution of spin relaxation rate of the samples. This was done to capture the vacancy and clustering kinetics, which occurs at a suitably slow rate somewhat below room temperature.

We have interpreted the measured relaxation spectra using a Monte Carlo simulation, in which four fitting parameters were employed: the dipolar width (Δ), trapping rate (ν_t), detrapping rate (ν_d), and fraction of initially trapped muons (P_0) [13, 16]. This method has been introduced in the literature [17-18]. An ensemble of 60 million muons are simulated to produce a five-dimensional relaxation function $f(\Delta, \nu_t, \nu_d, P_0, t)$, in which a muon spin is assumed to depolarize only when it is trapped, but no relaxation occurs during diffusion (two state model). Simulated relaxation functions are compared with the experimental ones to extract the best-fit parameters.

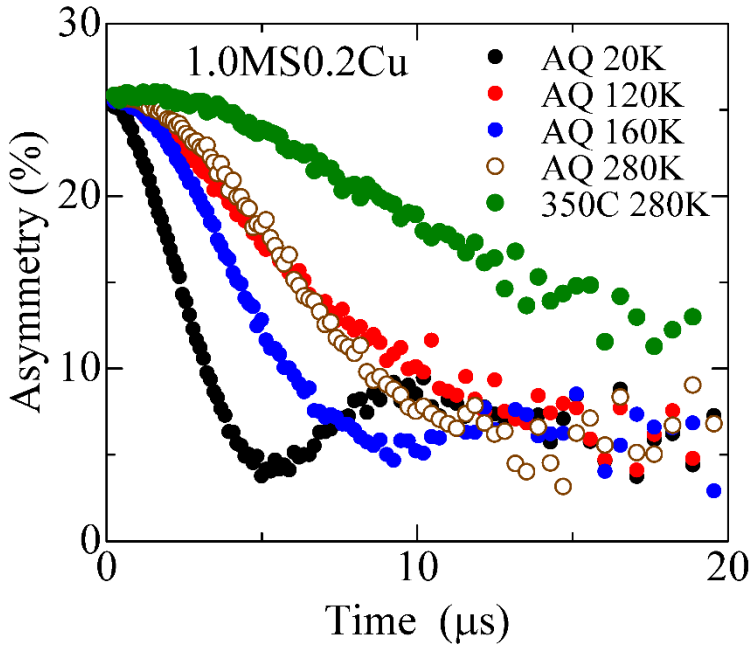

Figure 1: Example muon spin relaxation spectra for sample 1.0MS0.2Cu, showing spin asymmetry as a function of time spent inside the sample before muon decay.

Figure 1 shows the zero-field relaxation spectra observed for 1.0MS0.2Cu-AQ at measurement temperatures 20–280 K (−253 to 7 °C) and for 1.0MS0.2Cu-350C at 280 K (7 °C). The horizontal axis denotes the time (t) from a muon pulse was injected into the sample until the muon decay. The plot demonstrates that the muon spin depolarization rate depends heavily on temperature. The spectrum for 1.0MS0.2Cu-AQ at 20 K (−253 °C), where the kinetics are very slow, has a typical shape described by the Kubo–Toyabe function [19]:

$$G(t) = \frac{1}{3} + \frac{2}{3}(1 - \Delta^2 t^2) e^{-\frac{1}{2}\Delta^2 t^2}, \qquad (1)$$

where Δ is the dipolar width. This function yields a minimum at $t = \sqrt{3}/\Delta$ and subsequent increase to an asymptotic asymmetry value. Assuming a simple magnetic dipole interaction between an aluminum nucleon ^{27}Al and a muon, Δ can be described as [20-21]:

$$\Delta^2 = \left(\frac{\mu_0}{4\pi}\right)^2 I(I+1) \left(\hbar \gamma_{Al} \gamma_{\mu}\right)^2 \frac{4}{9} \sum_i r_i^{-6}, \qquad (2)$$

where I = 5/2 is the nuclear spin of ^{27}Al, γ_{Al} = 6.98 × 10^7 rad/sT and γ_{μ} = 8.52 × 10^8 rad/sT are the gyromagnetic ratios of ^{27}Al and muon, respectively, and r_i is the distance between the muon and all nearby ^{27}Al nuclei. If a muon is trapped at a tetrahedral site, this results in a Δ value of 0.49 μs^{-1}, while in an octahedral site, the Δ value is 0.38 μs^{-1}. These values are approximate and based on a rigid Al lattice: For exact values, the repulsion between the muon

and all surrounding atoms must be taken into account. In Al–Mg–Si(–Cu) alloy samples, Al nuclei dominate the dipole field which causes the muon spin relaxation, while contributions from Mg and Si nuclei are negligibly small, since naturally abundant ^{24}Mg and ^{28}Si nuclei have no magnetic moment. The naturally abundant ^{63}Cu and ^{65}Cu have comparable nuclear magnetic moments with that of ^{27}Al, therefore zero-field muon spin relaxation spectra in pure copper showed a Δ value of approximately 0.39 μs^{-1} [22]. In this sense, a larger Δ value means that the muon is surrounded by a higher number of Al/Cu atoms. The relaxation speed, however, depends not only on Δ, but on the trapping, detrapping and diffusion rates of muons, which are dependent on the concentration of defects (e.g. vacancies), their binding energy with muons, and temperature.

Figure 1 further shows that the depolarization for 1.0MS0.2Cu-AQ at 120 K (−153 °C) is slower than that at 160 K (−113 °C), and the depolarization for 1.0MS0.2Cu-AQ at 280 K (7 °C) is faster than that for 1.0MS0.2Cu-350C at 280 K (7 °), reflecting a shift towards deeper traps with lower number densities as the temperature increases. Similar relaxation spectra were acquired for all samples listed in Table 1, and fit to simulated spectra, as described in section 2.

The fitting results of the trapping rates (v_t) for the samples are plotted as a function of temperature in Figure 2. The temperature variations of v_t in Figure 2(a) verify the three regions: 1) a low *T* region of 20–120K (−253 to −153 °C), 2) a mid *T* region of 140–200 K (−133 to −73 °C) and 3) a high *T* region of 220–300K (−53 to +27 °C). In the low *T* region, it is known that muons are trapped in shallow electrical potentials produced by atoms in solid solution, primarily Mg [13, 16, 23-24]. This is evident from the fact that the v_t variation for 1.0Mg-10d resemble quite well those of the other samples at low *T*. The fitted Δ values at 20 K (−253 °C) for all the samples in Figure 2(a) were found to be approximately 0.35 μs^{-1}, similar to the measurement by Hatano et al. [17]. With one solute atom next to the muon, Eq. 2 matches the measurement for either a tetrahedral or octahedral site depending on its influence on the surrounding atom positions. The chemical properties of a positive muon are similar to that of a proton (hydrogen ion). A recent density functional theory calculation has proposed that a hydrogen prefers to be in the tetrahedral site in aluminum [25]. Therefore, muons are also expected to be trapped in the tetrahedral sites.

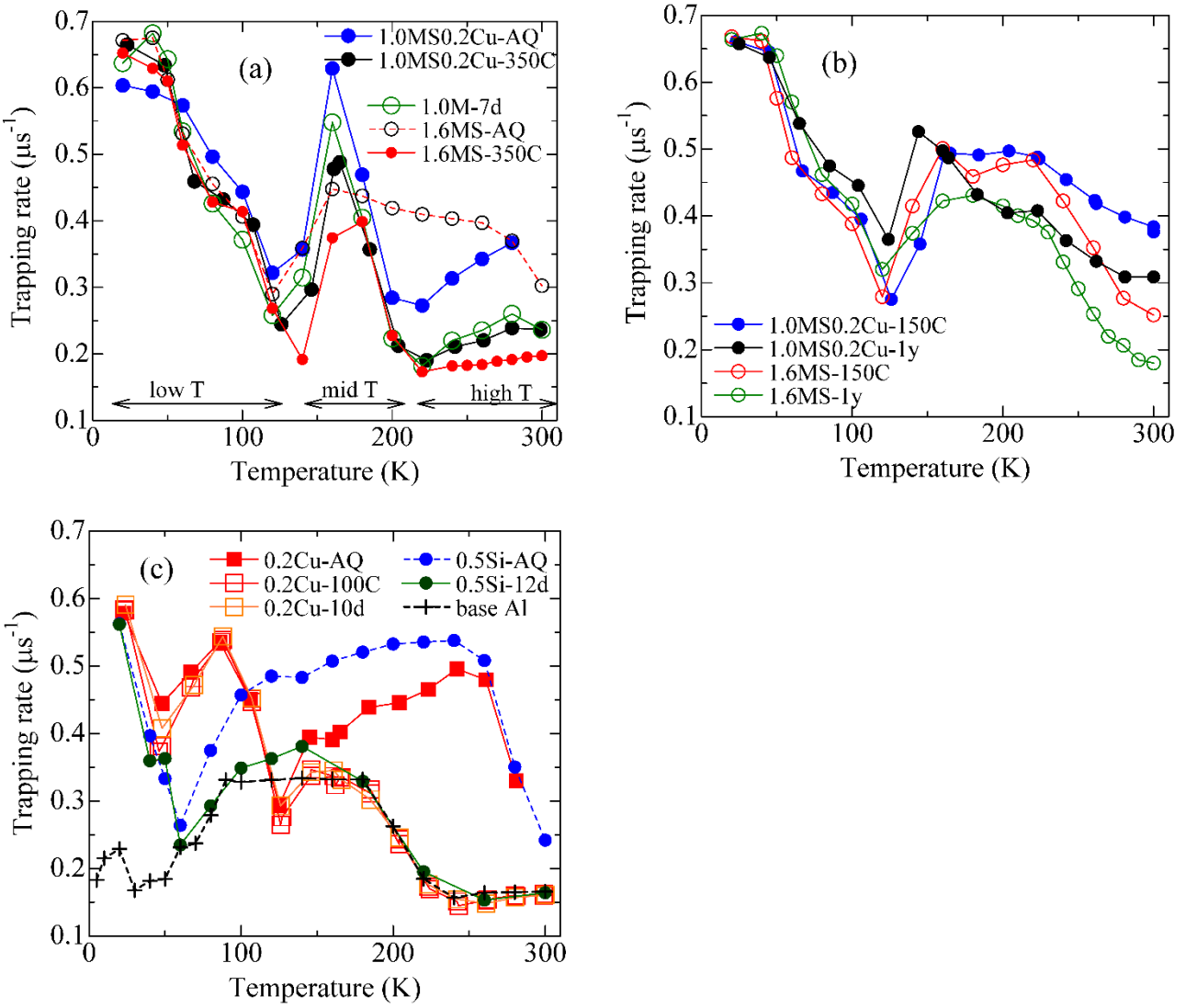

Figure 2: Best-fit trapping rates for relaxation spectra acquired at increasing temperatures from 20 K to 300 K (−253 °C to +27 °C). (a) The Al–Mg–Si(–Cu) alloy as quenched and aged at 623 K (350 °C), as well as binary (Al–Mg) and ternary (Al–Mg–Si) alloy samples for reference. (b) Al–Mg–Si(–Cu) samples thermally aged at 423 K (150 °C) and room temperature stored for 1 year. (c) Binary Al–Cu and Al–Si alloys, and pure aluminium.

In the mid *T* region, a sharp trapping rate peak at 160 K (−113 °C) emerged for 1.0MS0.2Cu-AQ, -350C and 1.0Mg-7d. This peak is most likely associated with small Mg clusters, since 1.0Mg-10d contains only dissolved Mg atoms. The electrical potentials produced by single dissolved Mg atoms are too shallow to trap muons in this *T* region. The fitted Δ values for 1.0MS0.2Cu at 120 K and 160 K (−153 and −113 °C) were found to assume the same value of 0.26 μs^{-1}. This Δ value, further decreased from that of pure Al, means that the muon is trapped by a complex of solute atoms/vacancies. The peak at 160 K (−113 °C) appears more strongly in the Al–Mg–Si–Cu alloy than in the ternary Al–Mg–Si alloy, which may be explained as follows: Through the precipitation sequence, we find more Si-rich

phases when Cu is added. This is exemplified by the equilibrium phases present in the samples annealed at 350 °C (623 °C), which are mainly β–Mg_2Si for 1.6MS and Q–$Mg_8Si_7Al_4Cu_2$ for 1.0MS0.2Cu. If all available Si goes into Q particles in 1.0MS0.2Cu-350C, the matrix still contains 0.28 at.% Mg and 0.10 at.% Cu, which can still form small clusters.

In the high *T* region, the v_t of the as quenched samples are the largest, whereas those of samples annealed at high temperatures are the smallest. In this region, muons are mainly trapped by vacancies, possibly bound to solute atoms [17]. The v_t values of 1.0MS0.2Cu-AQ are smaller than those of 1.6MS-AQ in the high T region, but the measurement points at the highest temperatures seem to indicate 1.0MS0.2Cu-AQ will take over with a higher trapping rate at 300 K (27 °C) and above. Following our earlier interpretation [16], the Cu-free alloy has a higher number density of solute clusters (trapping muons at 150–250 K (−123 to −23 °C)), while the Cu-added alloy has a higher number density of vacancies (trapping muons above 250 K (−23 °C)). It has been widely noticed that Cu addition to Al–Mg–Si alloys delay the precipitation processes, especially in the early stage of natural aging [26-28]. Even in the as quenched condition, the two samples were exposed to natural aging for 10–15 minutes, during which the cluster formation (especially Si–vacancy complex formation) proceeds with a lower speed if the Cu concentration is higher.

The artificial aging and long-term natural aging effects on v_t are seen for 1.0MS0.2Cu and 1.6MS in Figure 2(b). In the high-temperature region (above 200 K (−73 °C)), 1.0MS0.2Cu have higher trapping rates than its Cu-free counterpart. Adding Cu has the effect of retaining a high number density of vacancies in the material even after annealing or long-time room temperature storage. A rebalancing at medium temperature is also occurring: From the as-quenched conditions in Figure 2(a), the sharp peak at 160 K (−113 °C) (Mg atoms/clusters) is replaced by a broader peak at 140–220 K (−133 to −53 °C) (larger solute-vacancy clusters). This broad peak is already present in 1.6MS-AQ, which means the early clustering kinetics is significantly faster in the Cu-free alloy. This phenomenon has been observed before and explained by the large binding energy between Cu and vacancies, and the small diffusivity of Cu in aluminum [26]. A delayed clustering process in Cu added samples eventually lead to a high number density of small size clusters. It is worth to mention that the v_t values for 1.0MS0.2Cu-150C and -1y decreases with measurement temperature in an almost parallel manner above 200 K (−73 °C), and the same is valid for 1.6MS.

The temperature dependences of v_t for the binary alloys displayed in Figure 2(c) are rather different from those for the ternary and quaternary alloys. For the 0.2Cu samples, the changes in trapping rate with heat treatment happens at measurement temperatures above 120 K (−153 °C). There is a unique, constant trapping rate peak for Al–Cu at 80 K, which have been explained by (vacancy-free) Cu atom complexes trapping muons [29]. This is comparable to the peak at 160 K (−113 °C) for Mg atoms seen in Figure 2(a). The high v_t values at 20 K (−253 °C) for 0.2Cu and 0.5Si are caused by single Cu/Si impurity atoms. Above 120 K (−153 °C), the large v_t values of 0.2Cu-AQ are naturally attributable to Cu–vacancy pairs and complexes. Both natural and artificial aging for Al–0.2% Cu completely suppresses the high-temperature behavior, reducing the v_t values to base Al levels. This heat treatment response is similar to that of Al–0.5% Si, although the starting point is different: 0.5Si-AQ has an elevated trapping rate at lower temperatures (down to 60 K (−213 °C)). The main result of Figure 2(c) is that vacancies are annealed out of Al–Cu

and Al–Si alloys if subjected to either natural or artificial aging. For Al–Mg, a higher temperature is required to achieve this [16], while in the binary and ternary alloys presented in Figures 2(a,b), the temperature must be high enough to dissolve coherent precipitates, around 623 K (350 °C) for the vacancies to be freed.

From previous μSR studies, muons are considered to be trapped by single vacancies or vacancy–solute pairs near room temperature. The ν_t values, therefore in most cases, decreases with time during natural aging since excess vacancies are lost at imperfections, such grain boundaries, voids, surfaces, etc. The change in trapping rate during storage at 280 K (7 °C) after quenching was measured for 1.0MS0.2Cu, 1.6MS, 0.5Si, 0.2Cu and base Al, as shown in Figure 3. The horizontal axis denotes the time after quenching from SHT on a logarithmic scale. The ν_t values for 1.6MS, 0.5Si, 0.2Cu and base Al decreases with time. The speed of the decrease is inversely correlated with the solute concentration, as is expected since muons have more defects to be trapped at and more time to undergo spin relaxation. The reason why the ν_t values of 0.2Cu start out lower than in the other alloys is unclear.

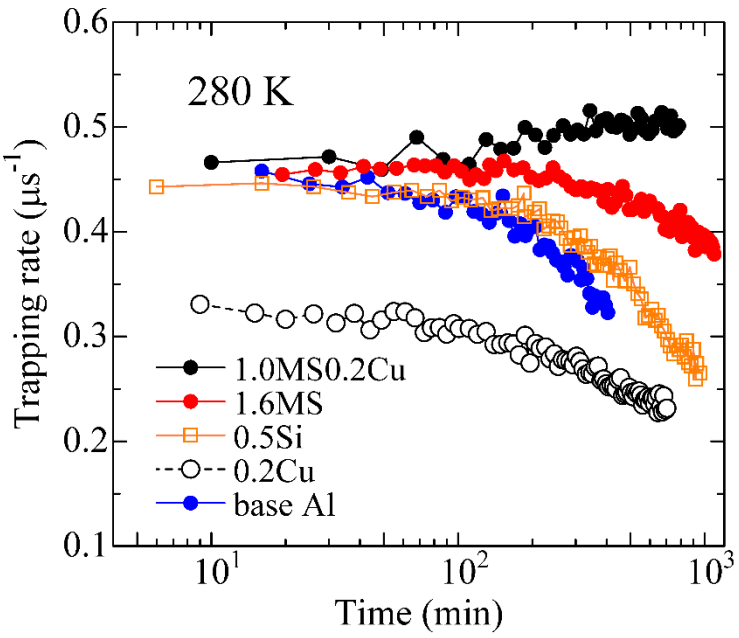

Figure 3: Fitted trapping rates from isotheral relaxation spectra. Samples are quenched from SHT and kept at 280 K (7 °C) throughout the measurements. The trapping rates decrease with time for all alloys except the quaternary Al–Mg–Si–Cu alloy, which increases with time.

The surprising result from the isothermal experiment is that the ν_t value for 1.0MS0.2Cu increases with time. The reproducibility of this trend was checked by conducting three individual isothermal runs, that turned out consistent. If muons are trapped only at vacancy associated sites, the result indicates that the number density of vacancies *increases* with time after quenching when all elements Mg, Si and Cu are present in the alloy composition. This suggests that new vacancies are continuously diffusing into the material and binding to solute atoms, shifting the

equilibrium concentration of vacancies to higher levels than in the alloys with fewer elements. For this to be possible, vacancy–solute bonds must be much more energetically favorable to form in 1.0MS0.2Cu than in 1.6MS. As reported in literature, Cu has the largest binding energy with vacancies among the solute elements and an attractive interaction with Mg atoms [26, 28, 30-32]. Since the effect does not occur in binary Al–Cu, several elements must interact, which suggests that also small vacancy-rich clusters (containing at least 2–3 solute atoms) can trap vacancies at 280 K (7 °C). Depending on the role of Si, a similar increase in vacancy concentration might also happen in ternary Al–Mg–Cu alloys, which have not been studied with μSR yet.

The early cluster formation kinetics in Al-Mg-Si alloys are slow in the presence of Cu [26], such that the clusters in Al–Mg–Si–Cu alloys, stay small in size for a long time at room temperature. This means a higher density of clusters in Cu-added alloys, and a higher tendency to contain vacancies. Meanwhile, clusters in Al–Mg–Si grow large and do not bind vacancies as well, a behavior that can be prevented with short pre-aging treatments at e.g. 343–373 K (70–100 °C) after SHT [11, 16]. The presence of vacancies inside clusters can be crucial for a good aging response: when clusters transform into crystalline precipitates during artificial aging, the vacancies are freed and can again act as nucleation points for further clusters and precipitates.

Muon spin relaxation experiments were performed on an Al–Mg–Si–Cu alloy and ternary/binary references to investigate the effect of Cu on Mg–Si-clustering kinetics. As we increase the sample temperature from 20 K to 300 K (from −253 °C to +27 °C), we probe defects of lower densities and higher binding muon trapping potentials, starting with single atoms and going through small atomic clusters and vacancies bound in clusters/precipitates, finally ending up at vacancy–solute pairs and small vacancy-rich clusters at room temperature. This enables us to make the following observations:

- When quenching a binary aluminium alloy from solution heat treatment (SHT), most of the vacancies have escaped from Al–Si and Al–Cu after a few days at room temperature, while Al–Mg retains vacancies until a heat treatment at 473 K (200 °C) is conducted, due to stable Mg–vacancy bonds. Temperatures of 623 K (350 °C) are required to anneal the vacancies out of Al–Mg–Si(–Cu) alloys.

- Natural aging has a negative effect on the strength response upon artificial aging of Al–Mg–Si alloys, but this is prevented by adding Cu. Our results indicate that this is caused by the quick formation and growth of atomic clusters and loss of quenched-in vacancies in Al–Mg–Si, while a high concentration of smaller, more vacancy-rich clusters are produced in Al–Mg–Si–Cu.

- In Al–Mg–Si–Cu alloys (but not Al–Cu or Al–Mg–Si alloys), the vacancy concentration even increases during room temperature storage, because very stable Mg–Cu–vacancy configurations raises the equilibrium concentration of vacancies in the material. All the alloying elements (possibly except Si) must be present in order for the binding energy with vacancies to be sufficient to produce this effect.

Acknowledgments

This study has been supported by JSPS KAKENHI (Grant Number JP18H01747), The Norwegian–Japanese Aluminium alloy Research and Education Collaboration (INTPART), project number 249698, and The Japan Institute of Light Metals.

References

1. A. Serizawa, S. Hirosawa and T. Sato, *Metallurgical and Materials Transactions A* 2008, vol. 39, pp. 243-251.
2. F. De Geuser, W. Lefebvre and D. Blavette, *Philosophical Magazine Letters* 2006, vol. 86, pp. 227-234.
3. K. Matsuda, A. Kawai, K. Watanabe, S. Lee, C.D. Marioara, S. Wenner, K. Nishimura, T. Matsuzaki, N. Nunomura, T. Sato, R. Holmestad and S. Ikeno, *Mater Trans* 2017, vol. 58, pp. 167-175.
4. S. Wenner, C.D. Marioara, S.J. Andersen and R. Holmestad, *Int J Mater Res* 2012, vol. 103, pp. 948-954.
5. F.A. Martinsen, F.J.H. Ehlers, M. Torsæter and R. Holmestad, *Acta Mater* 2012, vol. 60, pp. 6091-6101.
6. J. Banhart, C.S.T. Chang, Z. Liang, N. Wanderka, M.D.H. Lay and A.J. Hill, *Advanced Engineering Materials* 2010, vol. 12, pp. 559-571.
7. D.J. Chakrabarti and D.E. Laughlin, *Progress in Materials Science* 2004, vol. 49, pp. 389-410.
8. K. Matsuda, S. Ikeno, Y. Uetani and T. Sato, *Metallurgical and Materials Transactions A* 2001, vol. 32, pp. 1293-1299.
9. C.D. Marioara, S.J. Andersen, T.N. Stene, H. Hasting, J. Walmsley, A.T.J. Van Helvoort and R. Holmestad, *Philos Mag* 2007, vol. 87, pp. 3385-3413.
10. J. Kim, E. Kobayashi and T. Sato, *Mater Trans* 2015, vol. 56, pp. 1771-1780.
11. J. Kim, E. Kobayashi and T. Sato, *Mater Trans* 2011, vol. 52, pp. 906-913.
12. P. Dumitraschkewitz, S.S.A. Gerstl, P.J. Uggowitzer, J.F. Löffler and S. Pogatscher, *Advanced Engineering Materials* 2017, vol. 19, p. 1600668.
13. S. Wenner, R. Holmestad, K. Matsuda, K. Nishimura, T. Matsuzaki, D. Tomono, F.L. Pratt and C.D. Marioara, *Phys Rev B* 2012, vol. 86.
14. A. Yaouanc and P.D. de Réotier: *Muon Spin Rotation, Relaxation, and Resonance: Applications to Condensed Matter*. OUP Oxford, 2011.
15. T. Matsuzaki, K. Ishida, K. Nagamine, I. Watanabe, G.H. Eaton and W.G. Williams, *Nuclear Instruments and Methods in Physics Research Section A: Accelerators, Spectrometers, Detectors and Associated Equipment* 2001, vol. 465, pp. 365-383.
16. S. Wenner, K. Nishimura, K. Matsuda, T. Matsuzaki, D. Tomono, F.L. Pratt, C.D. Marioara and R. Holmestad, *Acta Mater* 2013, vol. 61, pp. 6082-6092.
17. T. Hatano, Y. Suzuki, M. Doyama, Y.J. Uemura, T. Yamazaki and J.H. Brewer, *Hyperfine Interactions* 1984, vol. 17, pp. 211-217.
18. E. Sato, T. Hatano, Y. Suzuki, M. Imafuku, M. Sunaga, M. Doyama, Y. Morozumi, T. Suzuki and K. Nagamine, *Hyperfine Interactions* 1984, vol. 17, pp. 203-209.
19. R.S. Hayano, Y.J. Uemura, J. Imazato, N. Nishida, T. Yamazaki and R. Kubo, *Phys Rev B* 1979, vol. 20, pp. 850-859.
20. A. Schenck: *Muon spin rotation spectroscopy*. Taylor and Francis Inc, Philadelphia, PA (USA), 1985.
21. T. Yamazaki, *Hyperfine Interactions* 1979, vol. 6, pp. 115-125.
22. R. Kadono, J. Imazato, T. Matsuzaki, K. Nishiyama, K. Nagamine, T. Yamazaki, D. Richter and J.M. Welter, *Phys Rev B* 1989, vol. 39, pp. 23-41.
23. K. Nishimura, K. Matsuda, R. Komaki, N. Nunomra, S. Wenner, R. Holmestad, T. Matsuzaki, I. Watanabe and F.L. Pratt, *Arch Metall Mater* 2015, vol. 60, pp. 925-929.
24. O. Hartmann, E. Karlsson, E. Wäckelgrd, R. Wäppling, D. Richter, R. Hempelmann and T.O. Niinikoski, *Phys Rev B* 1988, vol. 37, pp. 4425-4440.

25. L. Ismer, M.S. Park, A. Janotti and C.G. Van de Walle, *Phys Rev B* 2009, vol. 80, p. 184110.
26. M. Liu and J. Banhart, *Materials Science and Engineering: A* 2016, vol. 658, pp. 238-245.
27. M. Werinos, H. Antrekowitsch, T. Ebner, R. Prillhofer, P.J. Uggowitzer and S. Pogatscher, *Mater Design* 2016, vol. 107, pp. 257-268.
28. M.W. Zandbergen, Q. Xu, A. Cerezo and G.D.W. Smith, *Acta Mater* 2015, vol. 101, pp. 136-148.
29. W.J. Kossler, A.T. Fiory, W.F. Lankford, J. Lindemuth, K.G. Lynn, S. Mahajan, R.P. Minnich, K.G. Petzinger and C.E. Stronach, *Physical Review Letters* 1978, vol. 41, pp. 1558-1561.
30. D. Hatakeyama, K. Nishimura, K. Matsuda, T. Namiki, S. Lee, N. Nunomura, T. Aida, T. Matsuzaki, R. Holmestad, S. Wenner and C.D. Marioara, *Metallurgical and Materials Transactions A* 2018.
31. P. Lang, Y.V. Shan and E. Kozeschnik, *Materials Science Forum* 2014, vol. 794-796, pp. 963-970.
32. P. Lang, T. Weisz, M.R. Ahmadi, E. Povoden-Karadeniz, A. Falahati and E. Kozeschnik, *Advanced Materials Research* 2014, vol. 922, pp. 406-411.
33. S. Wenner, K. Nishimura, K. Matsuda, T. Matsuzaki, D. Tomono, F.L. Pratt, C.D. Marioara and R. Holmestad, *Metall Mater Trans A* 2014, vol. 45a, pp. 5777-5781.

Figures and tables

Figure 1: Example muon spin relaxation spectra for sample 1.0MS0.2Cu, showing spin asymmetry as a function of time spent inside the sample before muon decay.

Figure 2: Best-fit trapping rates for relaxation spectra acquired at increasing temperatures from 20 K to 300 K (−253 °C to +27 °C). (a) The Al–Mg–Si(–Cu) alloy as quenched and aged at 623 K (350 °C), as well as binary (Al–Mg) and ternary (Al–Mg–Si) alloy samples for reference. (b) Al–Mg–Si(–Cu) samples thermally aged at 423 K (150 °C) and room temperature stored for 1 year. (c) Binary Al–Cu and Al–Si alloys, and pure aluminium.

Figure 3: Fitted trapping rates from isotheral relaxation spectra. Samples are quenched from SHT and kept at 280 K (7 °C) throughout the measurements. The trapping rates decrease with time for all alloys except the quaternary Al–Mg–Si–Cu alloy, which increases with time.

TABLE 1: All samples used in this work. The sample composition (Al balanced), heat treatment after SHT and abbreviated labels for the samples are listed. A reference is given in cases where the samples have been used in earlier publications. RT means room temperature; AQ denotes “as quenched.”

Composition (at. %)	**Heat treatment**	**Label**	**Reference**
1.07 % Mg, 0.53 % Si	~15 min @ RT	1.6MS-AQ	[16, 23]
"	1 year @ RT	1.6MS-1y	[23]
"	1000 min @ 423 K (150 °C)	1.6MS-150C	[16, 23, 33]
"	30 min @ 623 K (350 °C)	1.6MS-350C	[33]
0.66 % Mg, 0.33 % Si, 0.2 % Cu	~10 min @ RT	1.0MS0.2Cu-AQ	
"	1 year @ RT	1.0MS0.2Cu-1y	
"	1000 min @ 423 K (150 °C)	1.0MS0.2Cu-150C	
"	30 min @ 623 K (350 °C)	1.0MS0.2Cu-350C	
1.0 % Mg	7 days @ RT	1.0Mg-7d	
0.5 % Si	~15 min @ RT	0.5Si-AQ	[16]
"	12 days @ RT	0.5Si-12d	[16]
0.2 % Cu	~10 min @ RT	0.2Cu-AQ	
"	10 days @ RT	0.2Cu10d	
"	1000 min @ 373 K	0.2Cu-100C	

	(100 °C)		
Pure Al, 0.01 % trace elements	66 days @ RT	base Al	[16, 23, 33]

310